A Volatile Organic Compound Sensor Using Porous Co_3O_4 Spheres

Tae-Hyung Kim, Ji-Wook Yoon, and Jong-Heun Lee[†]

Department of Materials Science and Engineering, Korea University, Seoul 02841, Korea

ABSTRACT

Porous Co_3O_4 spheres with bimodal pore distribution (size: 2-3 nm and ~ 30 nm) were prepared by ultrasonic spray pyrolysis of aqueous droplets containing Co-acetate and polyethylene glycol (PEG), while dense Co_3O_4 secondary particles with monomodal pore distribution (size: 2-3 nm) were prepared from the spray solution without PEG. The formation of mesopores (~ 30 nm) was attributed to the decomposition of PEG. The responses of a porous Co_3O_4 sensor to various indoor air pollutants such as 5 ppm C_2H_5OH, xylene, toluene, benzene, and HCHO at 200°C were found to be significantly higher than those of a commercial sensor using Co_3O_4 and dense Co_3O_4 secondary particles. Enhanced gas response of porous Co_3O_4 sensor was attributed to high surface area and the effective diffusion of analyte gas through mesopores (~ 30 nm). Highly sensitive porous Co_3O_4 sensor can be used to monitor various indoor air pollutants.

Key words : Gas sensor, Co_3O_4, Volatile organic compound, Spray pyrolysis

1. Introduction

An oxide semiconductor gas sensor detects a small quantity of explosive gases, environmental gases, toxic gases, etc. based on changes in resistance upon the reaction between the surface of sensing materials and analyte gases.[1] Gas sensing materials that have been researched include n-type oxide semiconductors such as SnO_2,[2] ZnO,[3] In_2O_3,[4] TiO_2,[5] etc. When oxygen adsorbs on the surface of an n-type oxide semiconductor and receives electrons near the surface, an electron depletion layer is formed with the sensor resistance increasing. When there are reducing gases in the atmosphere, the reaction between reducing gas and negatively charged adsorbed oxygen causes electrons to flow into an n-type oxide semiconductor, which decreasesthe sensor resistance. In contrast, the p-type oxide semiconductor gas sensor forms a hole accumulation layer on the surface when negatively charged oxygen is absorbed. Upon reaction between reducing gases and absorbed oxygen on the surface, electrons are discharged and recombined with the positive hole. As a result, the hole concentration near the surface decreases and the sensor resistance increases.[6]

Recently, p-type oxide semiconductors including NiO,[7] CuO,[8] Cr_2O_3,[9] and Co_3O_4[9,10] have been considered as gas sensors, but their low level of gas response limits the sensors applications. However, p-type oxide semiconductors feature the outstanding catalytic activity to various gases, and thus it is possible to measure gases that are difficult to

be measured by means of an n-type oxide semiconductor.[11] Thus, designing p-type oxide semiconductor gas sensors of outstanding gas response is of great importance. For a semiconductor gas sensor to achieve a high level of gas response and high response rates, nano structures that facilitate gas diffusion and involve large specific surface areas are advantageous such as nanowire networks,[12] hollow spheres,[4] and hierarchical structures.[3,4,10,13]

The ultrasonic spray pyrolysis is a process that facilitates forming spherical secondary particles through thermal decomposition of droplets in source solution. Upon adding carbon precursors that can be removed at high temperature, it is possible to prepare spherical secondary porous particles. In this study, spherical particles of porous Co_3O_4 with high specific surface areas are formed by means of ultrasonic spray pyrolysis, which is a method for highly sensitive detection to detect various pollutants in indoor environments.

2. Experimental Procedure

2.1 Co_3O_4 Composition

To compose porous Co_3O_4 spheres, 1.77 g of $(CH_3CO_2)_2Co$ (99.99$_5$%, Sigma-Aldrich Co., Ltd., USA) and 1 g of PEG (Polyethylene glycol, average molecular weight: 8000, Sigma-Aldrich Co., Ltd., USA) were dissolved and mixed in 500 ml of distilled water. A supersonic generator was utilized to generate droplets in source solution, and thermal decomposition was induced in a reaction furnace set to 700°C by means of a carrier gas (air, 40 L/min) in order to form a spherical precursor containing Co. The precursor was collected through a powder trap, which were converted into porous Co_3O_4 spheres by thermal treatment at 400°C for

[†]Corresponding author : Jong-Heun Lee
 E-mail : jongheun@korea.ac.kr
 Tel : +82-2-3290-3282   Fax : +82-2-928-3584

2 h in the air. In this process, PEGs were decomposed at high temperature, forming the porous structure. To examine the effect of the porous structure on the gas-sensing characteristics, Co_3O_4 nanoparticles and commercial Co_3O_4 fine particles went through thermal treatment with no PEG, and the gas-sensing characteristics were compared. Commercial Co_3O_4 particles were indicated as C-Co_3O_4, Co_3O_4 nanoparticles with no PEG NP-Co_3O_4, and porous Co_3O_4 particles with PEGs PEG-Co_3O_4 respectively.

2.2 Analysis

To analyze shapes of particles, a scanning electron field-emission microscope (FE-SEM, S-4300 Hitachi Co., Ltd., Japan) was utilized. For the phase analysis, an X-ray diffraction analyzer (XRD, Rigaku Model/MAX-2500, Source: CuKα) was used, and for the analysis of the specific surface area and pore distribution, Brunauer-Emmett-Teller method (BET, Tristar 3000, Micrometrics Co. Ltd., USA) was utilized.

2.3 Sensor Element Production and Measurement

The Co_3O_4 sensing materials were mixed with distilled water to be of a slurry formation, and the sensor elements were produced after being coated on alumina substrates where Au electrodes were patterned. The sensor elements were heat-treated for 2 h at 350°C by means of the heater installed at the back in order to remove residual water and stabilize them. The gas-sensing characteristics were then measured. The gas flow rate was fixed to 200 cm^3/min, and then the gas-sensing characteristics of six gases—5 ppm of C_2H_5OH, CO, p-xylene, toluene, benzene, and HCHO—were examined at 200, 250, and 300°C.

3. Results and Discussion

3.1 Shapes and Images of Composed Nano Particles

As for C-Co_3O_4, it was observed that primary particles as small as about 50 nm were agglomerated (Fig. 1(a), (b)). As for NP-Co_3O_4, secondary particles that were distorted and as small as 300-500 nm were observed. As spherical droplets passed through the high-temperature reaction furnace, the precursor of hollow spheres was formed. As it went through thermal treatment at higher temperature, the spherical form was damaged (Fig. 1(c), (d)). As for PEG-Co_3O_4 particles, the size was similar to that of NP-Co_3O_4, but the spherical form remained even after it passed through the high-temperature reaction furnace, which indicates that PEG elements functioned to maintain the spherical shape (Fig. 1(e), (f)). Yu et al.[14] produced fluorescent substances in the Pechini method by adding PEGs (molecular weight: 10,000), and the thermal analysis result shows that PEGs were decomposed at 358 and 378°C. Although spray pyrolysis temperature was 700°C in the present study, the reaction time at high temperature was relatively very short (< 3 s). Thus PEGs remained until the end of the spray pyrolysis, which maintained spherical shape. The
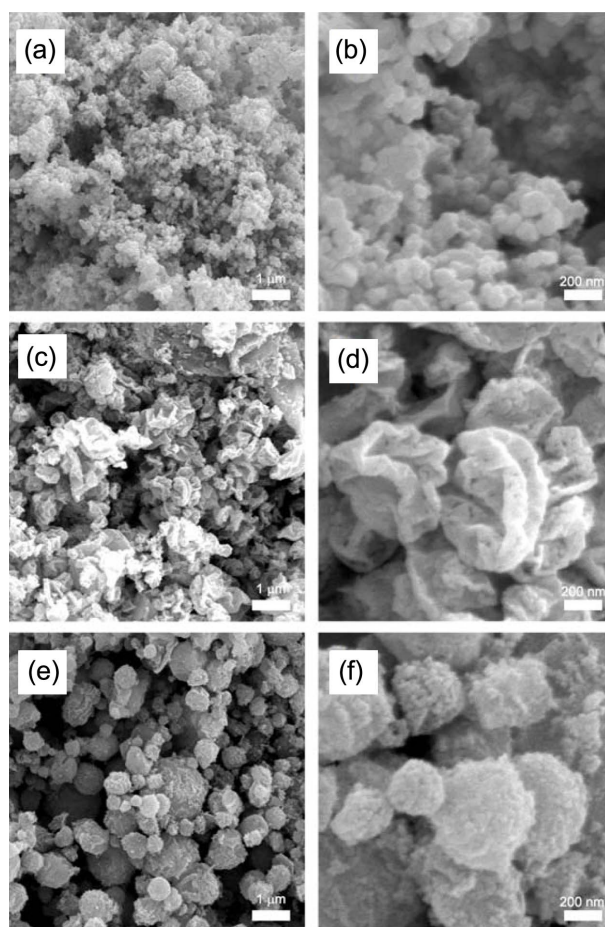
Fig. 1. Scanning electron microscopy (SEM) images of (a), (b) C-Co_3O_4, (c), (d) NP-Co_3O_4, (e), (f) PEG-Co_3O_4 powders after spray pyrolysis reaction and subsequent heat treatment at 400°C for 2 h.

XRD analysis shows that the three types of particles were in the spinel phase of Co_3O_4 (Fig. 2). Based on the Scherrer's equation, the primary particle sizes of C-Co_3O_4, NP-Co_3O_4, and PEG-Co_3O_4 were determined to be 43.1 nm ± 4.3 nm, 37.9 nm ± 3.0 nm, and 37.4 nm ± 4.0 nm respectively.

3.2 Analysis of Specific Surface Areas and Pore Distribution

To examine the pore distribution and specific surface area of each type of particles, the BET analysis was conducted (Fig. 3). The specific surface area of C-Co_3O_4 was 14.8 m^2/g, but the pore volume (size: 1 to 100 nm) is very small. The specific surface area of NP-Co_3O_4 particles was 24.9 m^2/g, which is larger than that of commercial particles. In addition, micro pores as small as 2-3 nm accounted for the large portion. As for PEG-Co_3O_4 particles, the specific surface area was 37.9 m^2/g, which is the largest. This was of a bimodal pore distribution where not only micro pores as small as 2 - 3 nm but also mesopores as small as 30 nm coexisted. 30 nm pores were observed in PEG-Co_3O_4 unlike NP-Co_3O_4, which can be explained by the pore generation

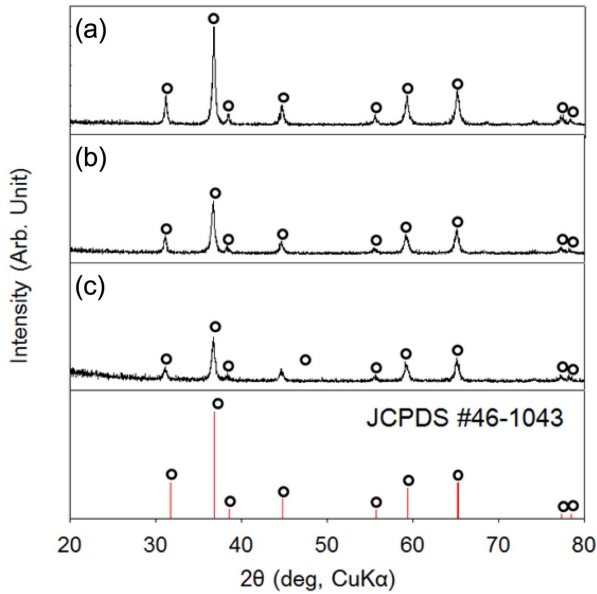**Fig. 2.** X-ray diffraction patterns of (a) C-Co_3O_4, (b) NP-Co_3O_4, (c) PEG-Co_3O_4 powders.
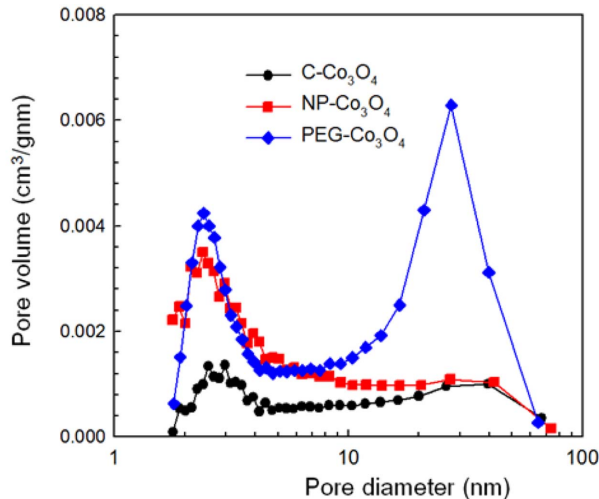

Fig. 3. Pore size distribution of C-Co_3O_4, NP-Co_3O_4, and PEG-Co_3O_4 powders.

upon the thermal decomposition of PEG elements at the end of the process while droplets with PEGs went through atomizing thermal decomposition.

3.3 Gas-sensing Characteristics Evaluation

When each Co_3O_4 sensor was exposed to 5 ppm of C_2H_5OH at 200°C, changes in sensor resistance were as shown in Fig. 4. When the three types of sensors—C-Co_3O_4, NP-Co_3O_4, and PEG-Co_3O_4—were exposed to C_2H_5OH, sensor resistance increased. Upon exposing to air, resistance decreased because of the gas-sensing characteristics of the p-type oxide semiconductor. Thus, the gas response was defined as R_g/R_a (R_g: resistance upon exposing to gases; R_a: resistance in the air). The gas responses of the three Co_3O_4
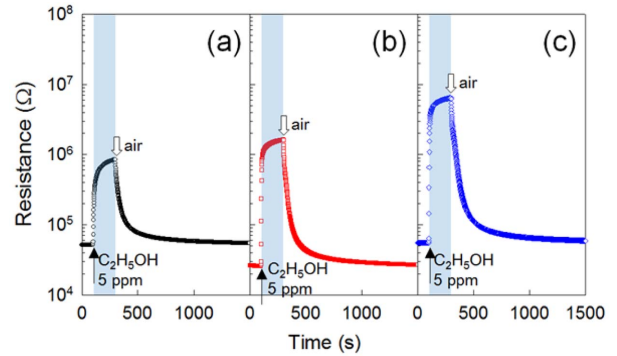

Fig. 4. Dynamic sensing transients of C-Co_3O_4, NP-Co_3O_4, and PEG-Co_3O_4 sensors to 5 ppm of C_2H_5OH at 200°C.
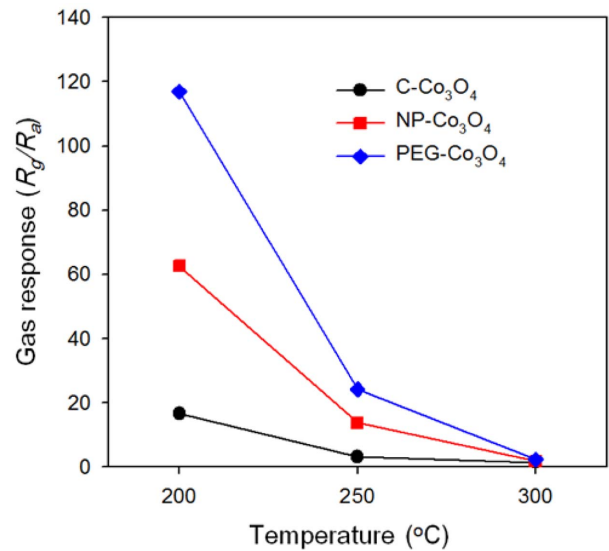

Fig. 5. Gas responses (R_g/R_a) to 5 ppm C_2H_5OH of C-Co_3O_4, NP-Co_3O_4, and PEG-Co_3O_4 sensors at 200 - 300°C.

sensors were compared in the range of 200-300°C (Fig. 5). All of the three sensors showed the highest response to C_2H_5OH at 200°C, and the figures were 16.7, 62.7, and 116.9 respectively. The response of PEG-Co_3O_4 to ethanol was about 7 times and twice higher than those of C-Co_3O_4 and NP-Co_3O_4 respectively.

As temperature increased thereafter, all of the three sensors involved drastic decrease of response even under 2 at 300°C. To determine the detection limit of PEG-Co_3O_4 sensors to C_2H_5OH, the response was measured at 200°C in the range of 0.5-5 ppm for each concentration level (Fig 6(b)). The response to 0.5 ppm of C_2H_5OH was as high as about 18.4. A linear regression analysis was conducted with $R_g/R_a > 1.2$ as the basic criterion for gas detection. The detection limit of C_2H_5OH was as low as 10 ppb (Fig. 6(b)). This indicates that PEG-Co_3O_4 sensors can detect even a quite small quantity of C_2H_5OH.

As for difference in the gas responses of the three sensors, the key paramters are the specific surface area, pore size /
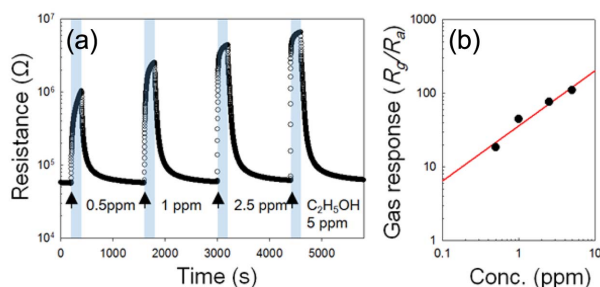
Fig. 6. (a) Sensing transients of PEG-Co$_3$O$_4$ to 0.5-5 ppm C$_2$H$_5$OH at 200°C, (b) gas response to C$_2$H$_5$OH as a function of concentration at 200°C.

Fig. 7. Gas response of (a) C-Co$_3$O$_4$, (b) NP-Co$_3$O$_4$, and (c) PEG-Co$_3$O$_4$ sensor to 5 ppm C$_2$H$_5$OH (E), CO (C), p-xylene (X), toluene (T), benzene (B), and HCHO (F) at 200°C.

volume distribution, and primary particle sizes. A hole accumulation layer near the surface of particles is responsible for chemiresistive reaction when a p-type oxide semiconductor reacted to gases. Thus, small primary particles are advantageous when it comes to high gas response. According to Scherrer's equation for the size of primary particles, the response of PEG-Co$_3$O$_4$/ NP-Co$_3$O$_4$ sensors was superior to that of C-Co$_3$O$_4$ sensors. However, PEG-Co$_3$O$_4$ and NP-Co$_3$O$_4$ sensors, which were of a similar primary particle size, showed a significantly different level of gas response. This indicates that there are other deciding factors of gas response.

It is reported that the size and distribution of pores within the gas-sensing film are closely related to the diffusion of analyte gases, and that the gas diffusion is one of the deciding factors of gas response.[15] For instance, when the sensing film is quite thick and the size of pores is very small, only small quantity of analyte gases can diffuse to the bottom of the film near electrodes, which decreases the gas response as a result. In addition, the size of pores affects the gas spreading mechanism significantly.

When the collisions between gas molecules become more important than collisions between gas molecules and pore walls, normal diffusion occurs. In contrast, mesopores whose pore size is as small as 2 to 50 nm involve Knudsen diffusion mainly upon collisions between gas molecules and pore walls. Knudsen diffusion constant (D$_k$) is known to be proportional to the size of pores for the same gas and at a constant temperature.[16] In other words, as the size of pores increases, gas diffusion is facilitated up to the point that the analyte gas effectively reaches all the way deep into the sensing film where there are electrodes. As a result, the gas response is enhanced. As for highly agglomerated C-Co$_3$O$_4$ particles, there are few pores among particles, and gas diffusion is minimized and the specific surface area is quite small. Therefore, the gas response is relatively low. As for NP-Co$_3$O$_4$, the specific surface area is relatively low, but the pores are as fine as 2-3 nm. Thus, the Knudsen diffusion coefficient is low and the analyte gas can hardly diffuse into the sensing film, which makes the gas response low. As for PEG-Co$_3$O$_4$, there are mesopores as big as 30 nm in addition
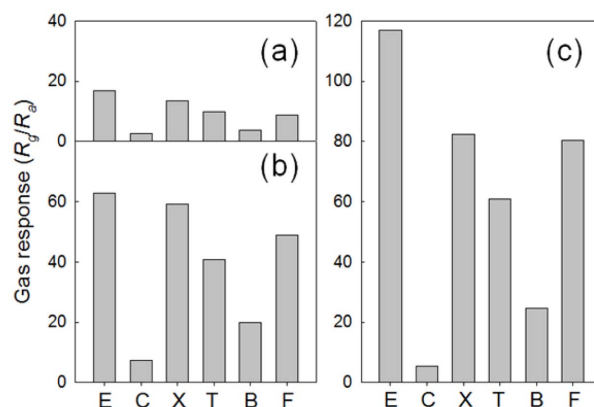
to those as small as 2 - 3 nm. According to the Knudsen diffusion coefficient proportional to the size of pores, the gas diffusion in PEG-Co$_3$O$_4$ can be 10 times better than that in NP-Co$_3$O$_4$. As PEGs are removed by thermal treatment, pores as big as 30 nm are generated, and these pores facilitate gas diffusion. In addition, as the specific surface area increases, gas response is improved drastically as well.

The responses to CO, p-xylene, toluene, benzene, and HCHO were measured at 200°C. The responses of PEG-Co$_3$O$_4$ sensor to all gases were substantially higher than that of C-Co$_3$O$_4$ and NP-Co$_3$O$_4$ sensors. In particular, the response to C$_2$H$_5$OH (R_g/R_a: 116.9), p-xylene (R_g/R_a: 82.3), toluene(R_g/R_a: 61), and HCHO (R_g/R_a: 80.5) significantly increased (Fig. 7).

Major pollutants of indoor environments include volatile organic compounds such as xylene, toluene, benzene, HCHO, C$_2$H$_5$OH, etc. While it is important to detect each environmental gas properly, it would be also quite advantageous if five different environmental pollutant gases can be measured with a similar level of response because only one sensor would be necessary to monitor the extent of indoor contamination.

There have been a lot of researches on n-type oxide semiconductor gas sensors. SnO$_2$, TiO$_2$, In$_2$O$_3$, Fe$_2$O$_3$, and WO$_3$ demonstrate a high response to C$_2$H$_5$OH. In contrast, their responses to other gases such as xylene, toluene, and benzene are so low that they are utilized mainly as alcohol sensors.[11] Co$_3$O$_4$ used in this study is a well-known catalyst to oxidize xylene and toluene.[17-19] This is consistent with the fact that the porous Co$_3$O$_4$ sensor in this study shows a relatively high level of responses to xylene, toluene, and benzene. Therefore, when porous Co$_3$O$_4$ (whose response to xylene, toluene, and benzene is outstanding) is used, it will be easier to measure the five major indoor pollutants with a single sensor.

4. Conclusions

In this study, porous Co_3O_4 spheres were prepared by ultrasonic spray pyrolysis, and the gas-sensing characteristics were evaluated. As for porous Co_3O_4 spheres where mesopores (formed by the decomposition of PEGs and as small as 30 nm) and micropores (as small as 2-3 nm) coexisted, the response to ethanol was about 7 times and 2 times better than that of commercial Co_3O_4 fine particles and Co_3O_4 nanoparticles prepared by pyrolysis of spray solution without PEG, respectively. This is probably because of the effective gas diffusion and large specific surface area of mesopores (30 nm). As a porous Co_3O_4 sensor has demonstrated a high responses to five major indoor environment gases (xylene, toluene, benzene, HCHO, and C_2H_5OH), it will be possible to monitor indoor contamination only by means of this single sensor.

Acknowledgments

REFERENCES

1. N. Yamazoe, "Toward Innovations of Gas Sensor Technology," *Sensor. Actuator. B Chem.*, **108** 2-14 (2005).

2. D. D. Vuong, G. Sakai, K. Shimanoe, and N. Yamazoe, "Highly Sensitive and Selective Gas Sensors Using Catalyst-Loaded SnO_2 Nanowires," *J. Sensor Sci. & Tech.*, **21** [3] 167-71 (2012).

3. K.-M. Kim, H.-R. Kim, K.-I. Choi, H.-J. Kim, and J.-H. Lee, "ZnO Hierarchical Nanostructures Grown at Room Temperature and their C_2H_5OH Sensor Applications," *Sensor. Actuator. B Chem.*, **155** 745-51 (2011).

4. K.-I. Choi, H.-R. Kim, and J.-H. Lee, "Enhanced CO Sensing Characteristics of Hierarchical and Hollow In_2O_3 Microspheres," *Sensor. Actuator. B Chem.*, **138** 497-503 (2009).

5. A. M. Ruiz, G. Sakai, A. Cornet, K. Shimanoe, and J. R. Morante, "Cr-doped TiO_2 Gas Sensor for Exhaust NO_2 Monitoring," *Sensor. Actuator. B Chem.*, **93** 509-18 (2003).

6. N. Barsan, C. Simion, T. Heine, and S. Pokhrel, "Modeling of Sensing and Transduction for P-type Semiconducting Metal Oxide Based Gas Sensors," *J. Electroceram.*, **25** 11-9 (2010).

7. N. G. Cho, H.-S. Woo, J.-H. Lee, and I.-D. Kim, "Thin-Walled NiO Tube Networks Functionalized with Catalytic Pt for Highly Selective C_2H_5OH Sensors Using Electrospun Fibers as a Sacrificial Template," *Chem. Commun.*, **47** 11300-2 (2011).

8. Y.-S. Kim, I.-S. Hwang, S.-J. Kim, C.-Y. Lee, and J.-H. Lee, "CuO Nanowire Gas Sensors for Air Quality Control in Automotive Cabin," *Sensor. Actuator. B Chem.*, **135** 298-303 (2008).

9. J.-W. Yoon, H.-J. Kim, H.-M. Jeong, and J.-H. Lee, "Gas Sensing Characteristics of P-type Cr_2O_3 and Co_3O_4 Nanofibers Depending on Inter-Particle Connectivity," *Sensor. Actuator. B Chem.*, **202** 261-71 (2014).

10. K.-I. Choi, H.-R. Kim, K.-M. Kim, D. Liu, G. Cao, and J.-H. Lee, "C_2H_5OH Sensing Characteristics of Various Co_3O_4 Nanostructures Prepared by Solvothermal Reaction," *Sens. Actuators B*, **143** 183-89 (2010).

11. H.-J. Kim and J.-H. Lee, "Highly Sensitive and Selective Gas Sensors Using P-type Oxide Semiconductors: Overview," *Sens. Actuators B*, **192** 607-27 (2014).

12. I.-S. Hwang, S.-J. Kim, J.-K. Choi, J.-J. Jung, D. J. Yoo, K.-Y. Dong, B.-K. Ju, and J.-H. Lee, "Large Scale Fabrication of Highly Sensitive SnO_2 Nanowire Network Gas Sensors by Single Step Vapor Phase Growth," *Sensor. Actuator. B Chem.*, **165** 97-103 (2012).

13. J.-H. Lee, "Gas Sensors Using Hierarchical and Hollow Oxide Nanostructures: Overview," *Sensor. Actuator. B Chem.*, **140** 319-36 (2009).

14. M. Yu, J. Lin, Z. Wang, J. Fu, S. Wang, H. J. Zhang, and Y. C. Han, "Fabrication, Patterning, and Optical Properties of Nanocrystalline YVO_4:A (A=Eu^{3+}, Dy^{3+}, Sm^{3+}, Er^{3+}) Phosphor Films via Sol-Gel Soft Lithography," *Chem. Mater.*, **14** 2224-31 (2002).

15. T. Hyodo, Y. Shimizu, and M. Egashira "Gas-Sensing Properties of Ordered Mesoporous SnO_2 and Effects of Coating Thereof," *Sens. Actuators B*, **93** 590–600 (2003).

16. G. Sakai, N. Matsunaga, K. Shimanoe, and N. Yamazoe, "Theory of Gas-Diffusion Controlled Sensitivity for Thin Film Semiconductor Gas Sensor," *Sensor. Actuator. B Chem.*, **93** 125-31 (2003).

17. H. J. Wu, L. D. Wang, Z. Y. Shen, and J. H. Zhao, "Catalytic Oxidation of Toluene and *P*-xylene Using Gold Supported on Co_3O_4 Catalyst Prepared by Colloidal Precipitation Method," *J. Mol. Catal. Chem.*, **351** 188-95 (2011).

18. Q. Yan, X. Li, Q. Zhao, and G. Chen, "Shape-Controlled Fabrication of the Porous Co_3O_4 Nanoflower Clusters for Efficient Catalytic Oxidation of Gaseous Toluene," *J. Hazard. Mater.,* **209–210** 385-91 (2012).

19. H.-M. Jeong, H.-J. Kim, P. Rai, J.-W. Yoon, and J.-H. Lee, "Cr-doped Co_3O_4 Nanorods as Chemiresistor for Ultraselective Monitoring of Methyl Benzene," *Sensor. Actuator. B Chem.*, **201** 482-89 (2014).